Amphiphiles Coordinated to Block Copolymers as a Template for Mesoporous Materials

Sami Valkama,[†] Teemu Ruotsalainen,[†] Harri Kosonen,[†,‡] Janne Ruokolainen,[†,§] Mika Torkkeli,[⊥] Ritva Serimaa,[⊥] Gerrit ten Brinke,*[,†,#] and Olli Ikkala*[,†]

Department of Engineering Physics and Mathematics and Center for New Materials, Helsinki University of Technology, P.O. Box 2200, FIN-02015 HUT, Espoo, Finland; VTT Microelectronics, Technical Research Centre of Finland, P.O. Box 1208, FIN-02044 VTT, Finland; Department of Materials, University of California Santa Barbara, Santa Barbara, California 93106; Department of Physics, University of Helsinki, P.O. Box 64, FIN-00014 Helsinki, Finland; and Laboratory of Polymer Chemistry, Materials Science Center, Dutch Polymer Institute, Nijenborgh 4, 9747 AG Groningen, The Netherlands

Received April 4, 2002; Revised Manuscript Received February 21, 2003

ABSTRACT: We show a concept where coordination of amphiphiles to one block of a block copolymer leads to polymeric supramolecules and self-organization and that mesoporous materials can be achieved with a dense set of polymer brushes at the surfaces upon cleaving the amphiphiles by extraction with a selective solvent. Polystyrene-*block*-poly(4-vinylpyridine) (PS-*block*-P4VP) is used with zinc dodecylbenzenesulfonate ($Zn(DBS)_2$) which can coordinate to the lone electron pairs of the pyridine nitrogens in the P4VP block, leading to complexes PS-*block*-P4VP$[Zn(DBS)_2]_y$. Coordination of $Zn(DBS)_2$ and structure formation were investigated using Fourier transformation infrared spectroscopy (FTIR), small- and wide-angle X-ray scattering (SAXS and WAXS), and transmission electron microscopy (TEM). Lamellar structure was observed and even points toward a structural hierarchy for high molecular weight block copolymers. FTIR, SAXS, and TEM showed that most of $Zn(DBS)_2$ can be extracted from such templates using methanol, leading to lamellar porous structures. P4VP brushes cover the resulting pore surfaces. The structures do not collapse probably due to the glassy PS and defects in the nonaligned structure. Compared to hydrogen bonding, coordination allows bonding of higher molecular weight amphiphiles due to the stronger attraction.

1. Introduction

Nature offers a variety of examples for membranes, where selectivity and functionality are achieved by a high density of pores with regular sizes and, more importantly, proper biochemical functionality at the pore walls. In synthetic materials, concepts to achieve controlled pore sizes have been reported, ranging from nanoporous (<20 Å), to mesoporous (20−500 Å), up to macroporous (>500 Å) materials (see recent reviews[1−4]). A classic concept is based on "track-etch" membranes, which is a useful platform for tailored materials.[1,5,6] Another example is provided by mesoporous ceramic materials based on sol−gel processing using surfactants.[7−9] Efforts to achieve nanoporous crystals based on packing constraints of robust molecular units, networks, and supramolecular design principles[10] have been described (see e.g. refs 3 and 11−19). In crystals, however, the pores tend to collapse upon emptying, as this allows more uniform packing density.

Polymers can have advantages to "lock" the porosity. Several methods have been presented based on for example assemblies of block copolymers in the synthesis of inorganic materials,[20−24] selective degradation processes,[25−27] rod−coil block copolymers,[28] honeycomb structures,[29,30] cross-linking hexagonally assembled amphiphiles,[31−34] and selective removal of hydrogen-bonded side chains (combs) from hierarchically self-organized polymeric comb−coil supramolecules.[35] The latter concept is based on the observation that "comb copolymer-like" structures[36−39] can be obtained using tailored physical interactions, and combining this structure into the block copolymer self-organization leads to hierarchical structures.[40−42]

Previously, it was observed that amphiphilic molecules can be hydrogen bonded to the pyridine groups of polystyrene-*block*-poly(4-vinylpyridine) (PS-*block*-P4VP), allowing structural hierarchy,[40,41] and mesoporous materials with cylindrical pores were demonstrated upon selective removal of the amphiphiles.[35] Here we wanted to use stronger physical interactions (*attraction*) between the amphiphiles and the block copolymer, enabling the use of higher molecular weight amphiphiles. This, in turn, could lead to higher porosity after selective removal of amphiphiles. We decided to use late transition metal zinc as a coordination center because it is known to form complexes with various polymers, including P4VP.[37,43−45] Accordingly, we used zinc dodecylbenzenesulfonate, $Zn(DBS)_2$. Zinc forms tetra- to hexacoordinated complexes, which means that Zn^{2+} may coordinate simultaneously to two or more pyridine rings, depending on the available steric freedom. In the polymeric complexes this may lead to an additional difficulty due to the cross-linking,[43] which may hinder the formation of highly ordered self-organized structures. $Zn(DBS)_2$ is also hygroscopic, and there is practically always expected to be some hydration water present in the samples.[46,47]

In the present work, the coordination between $Zn(DBS)_2$ and PS-*block*-P4VP is first studied to assess formation of the supramolecules PS-*block*-P4VP[Zn-

[†] Helsinki University of Technology.
[‡] VTT Microelectronics, Technical Research Centre of Finland.
[§] University of California, Santa Barbara.
[⊥] University of Helsinki.
[#] University of Groningen.
* Corresponding authors.

10.1021/ma020538k CCC: $25.00
Published on Web 05/07/2003

$(DBS)_2]_y$. The self-organization and its hierarchy in the solid state will also be investigated. Finally, the $Zn(DBS)_2$ molecules are cleaved, revealing mesoporous lamellar material allowing high surface area and a dense set of P4VP brushes at the lamellar walls.

2. Experimental Section

Materials. Two polystyrene-*block*-poly(4-vinylpyridine) (PS-*block*-P4VP) block copolymers were supplied by Polymer Source Inc., and they were used without further purification (high molecular weight ($M_{n,PS}$ = 238 100 g/mol, $M_{n,P4VP}$ = 49 500 g/mol, M_w/M_n = 1.23) and lower molecular weight ($M_{n,PS}$ = 41 400 g/mol, $M_{n,P4VP}$ = 1900 g/mol, M_w/M_n = 1.07)). Dodecylbenzenesulfonic acid (DBSA) was purchased from Tokyo Kasei (90%), and ZnO was acquired from J.T. Baker B. V. (99%). Zinc dodecylbenzenesulfonate $Zn(DBS)_2$ was synthesized in ethanol (Primalco Ltd., Finland, 99.5%) from DBSA and ZnO according to

$$ZnO + 2DBSA \rightarrow Zn(DBS)_2 + H_2O$$

The detailed description of the procedure is given elsewhere.[37] In contrast to the earlier work, the product was additionally purified by recrystallizing it three times from acetone (Riedel-de Häen, 99.5%). Finally, the $Zn(DBS)_2$ was dried in a vacuum (10^{-2} mbar) at 80 °C for 2 days.

Sample Preparation. The complexes PS-*block*-P4VP$[Zn(DBS)_2]_y$ were prepared by dissolving both components, PS-*block*-P4VP and $Zn(DBS)_2$, in chloroform (Riedel-de Häen, 99%). The number of $Zn(DBS)_2$ groups per 4-vinylpyridine repeat unit was denoted by y = 0, 0.6, 0.8, and 0.9. The solvent was slowly evaporated at 4 °C, and thereafter the samples were dried in a vacuum at 60 °C for 2 days and annealed in a vacuum at 150 °C for 24 h. The bulk samples were immersed in methanol (Riedel-de Häen, 99.8%) at room temperature for at least 12 h to remove $Zn(DBS)_2$ from the structures. To verify that $Zn(DBS)_2$ has been removed, SAXS, FTIR, and TEM measurements were performed again and compared to the original measurements.

Fourier Transformation Infrared Spectroscopy. FTIR spectroscopy was used to study the interaction between PS-*block*-P4VP and $Zn(DBS)_2$. All infrared spectra were obtained using a Nicolet Magna 750 FTIR spectrometer at room temperature. A minimum of 64 scans was averaged at a resolution of 2 cm^{-1}. The samples were analyzed from films cast on potassium bromide crystals. The solvent was evaporated in a vacuum at 60 °C for 24 h. After methanol extraction samples were dried in a vacuum at room temperature for 24 h and were grounded with KBr and then pressed to pellets.

X-ray Scattering. X-ray scattering was used to study the mesomorphic behavior and crystallinity of the samples. Most of the experiments were performed with a conventional sealed X-ray tube. The Cu Kα radiation (λ = 1.54 Å) was monochromatized by means of totally reflecting mirror (Huber small-angle chamber 701) and Ni filter. Sample-to-detector distances of 80, 170, and 1250 mm were used (q range between 0.008 and 2.00 $Å^{-1}$). Scattering intensities were measured using a 2-D area detector (Bruker AXS). The accessible q range was not sufficient for the high molecular weight block copolymer, and additional measurements were performed at the high-brilliance beamline ID2 of the European Synchrotron Radiation Facility (ESRF). The station has an undulator X-ray source with focusing optics. At 12.46 keV (λ = 0.995 Å) the flux of photons is about 10^{12} photons/s across the 0.2 × 0.2 mm^2 size beam. The distance between sample and detector was 10 m. The accessible scattering vector lengths range from 0.004 to 0.07 $Å^{-1}$. The detector was an X-ray image intensifier (TH 49-427) lens coupled to the ESRF developed two-dimensional CCD camera.

Transmission Electron Microscopy. Bulk samples of PS-*block*-P4VP$[Zn(DBS)_2]_y$ for TEM characterization were first embedded in epoxy and cured at 60 °C overnight. Ultrathin sections (approximately 70 nm) were cryomicrotomed at −120 °C. Methanol extracted samples were prepared as follows: Cryo-trimmed sample blocks were immersed in methanol for a few hours in order to remove $Zn(DBS)_2$. Thereafter, 70 nm thin sections were cryomicrotomed from these mesoporous specimens. Sections were picked up on 600 mesh copper grids, and to enhance contrast, some microtomed sections were stained in the vapor of I_2 crystals. Bright field TEM was performed on JEOL-1200EX and JEOL-2000FX transmission electron microscopes operated at an accelerating voltage of 60 kV and 200 kV, respectively.

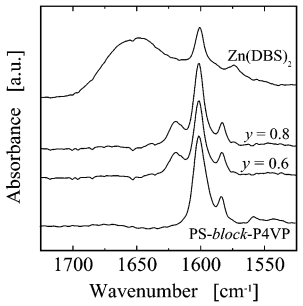

Figure 1. FTIR absorption bands for $Zn(DBS)_2$, PS-*block*-P4VP$[Zn(DBS)_2]_y$, and PS-*block*-P4VP. The formation of coordination bond is seen as a shift of the aromatic carbon−nitrogen stretching band from 1597 to ca. 1619 cm^{-1} when the pyridine group participates in metal−ligand π-bonding.

3. Results and Discussion

Evidence for the complex formation between $Zn(DBS)_2$ and PS-*block*-P4VP ($M_{n,PS}$ = 41 400 g/mol, $M_{n,P4VP}$ = 1900 g/mol) was obtained on the basis of the FTIR bands characteristic for the aromatic carbon−nitrogen stretching. Figure 1 shows the FTIR spectra of $Zn(DBS)_2$, selected PS-*block*-P4VP$[Zn(DBS)_2]_y$ complexes, and PS-*block*-P4VP in the 1725−1525 cm^{-1} region. PS-*block*-P4VP has a band occurring at ca. 1600 cm^{-1}, which is a combination of the aromatic carbon−carbon stretching band of the phenyl groups within PS and the aromatic carbon−nitrogen stretching band of the uncomplexed (i.e., free) pyridine rings within P4VP (1596−1597 cm^{-1}).[37,44,45] Pure $Zn(DBS)_2$ has an aromatic carbon−carbon stretching band at ca. 1600 cm^{-1} due to phenyl groups. Coordination of Zn^{2+} to pyridine is known lead to a shifted absorption to higher wavenumbers due to the metal−ligand π-bonding.[44,45] In agreement, in Figure 1 a new band is observed for the complexes PS-*block*-P4VP$[Zn(DBS)_2]_y$ at ca. 1619 cm^{-1}, confirming coordination. Upon increasing the mole fraction y of $Zn(DBS)_2$, the absorption band at 1619 cm^{-1} is expected to increase because more pyridine rings take part in the complex formation and at the same time the absorbance of the free pyridine rings at 1596−1597 cm^{-1} should gradually decrease until saturation is achieved. However, it was observed that the relative peak heights at 1619 cm^{-1} and near 1600 cm^{-1}, did not essentially change as a function of y when $y > 0.30$ (data not shown here). This is reasonable because each added $Zn(DBS)_2$ molecule increases also the absorption near 1600 cm^{-1} due to two added phenyl rings. In addition, more than one pyridine can be complexed to Zn^{2+} simultaneously, depending on the steric availability.[43] Similar FTIR behavior was also seen for the high molecular weight block copolymer complexes.

The TEM micrograph of PS-*block*-P4VP$[Zn(DBS)_2]_{0.9}$ using the high molecular weight block copolymer ($M_{n,PS}$ = 238 100 g/mol, $M_{n,P4VP}$ = 49 500 g/mol) indicates a lamellar structure with a periodicity of ca. 1100 Å (see Figure 2a). As no effort was made to align

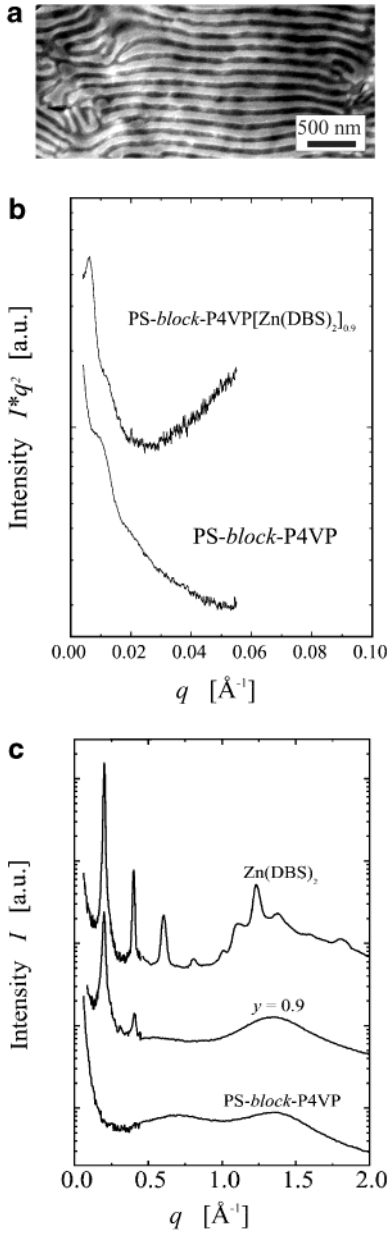

Figure 2. (a) TEM micrograph for PS-*block*-P4VP[Zn(DBS)$_2$]$_{0.9}$ showing a lamellar structure. The P4VP[Zn(DBS$_2$)]$_{0.9}$ domain shows dark due to the I_2 staining. X-ray intensity patterns for Zn(DBS)$_2$, PS-*block*-P4VP[Zn(DBS)$_2$]$_{0.9}$, and PS-*block*-P4VP in the (b) $q < 0.06$ Å^{-1} and (c) $q = 0.06-2.00$ Å^{-1} regions. The magnitude of the scattering vector is given by $q = (4\pi/\lambda) \sin \theta$, where 2θ is the scattering angle and $\lambda = 1.54$ Å. The curves have been shifted for clarity. The curves in (c) have been combined from two measurements having different sample-to-detector distances ($M_{n,PS} = 238\ 100$ g/mol, $M_{n,P4VP} = 49\ 500$ g/mol).

the local lamellar structures, they do not have a common orientation and a relatively large number of defects were observed, which incidentally turned useful to prevent the structures from collapsing upon removal of Zn(DBS)$_2$ at the final stage. Synchrotron SAXS shows a distinct peak at $q^* = 0.0060$ Å^{-1} and a faint shoulder at $2q^*$ (Figure 2b), which also supports a lamellar structure with a periodicity of ca. 1000 Å. By contrast, the uncomplexed PS-*block*-P4VP shows only a broad shoulder at slightly higher angles, probably due to the problems to achieve well-developed structures in pure high molecular weight block copolymers. The more distinct SAXS peak in PS-*block*-P4VP[Zn(DBS)$_2$]$_{0.9}$ may

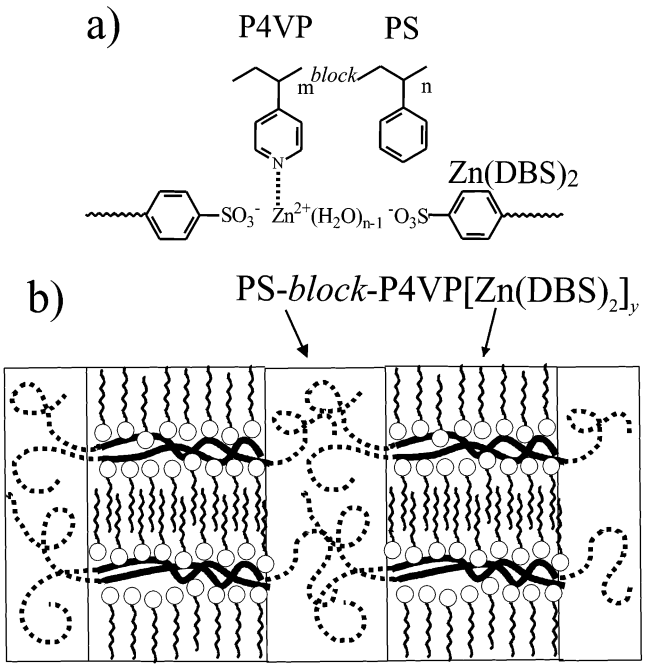

Figure 3. Schematic picture of the proposed coordination bonding between PS-*block*-P4VP and Zn(DBS)$_2$ and lamellar-*within*-lamellar structure of PS-*block*-P4VP[Zn(DBS)$_2$]$_{0.9}$. Note that Zn(DBS)$_2$ can be coordinated to more than one pyridine ring, however, still counterbalanced by the steric hindrances due to the polymer chains. Therefore, the actual coordination geometry is not known and is not addressed here. In addition, the scheme indicates that some hydration water may remain in the sample despite the drying.

be caused by an additional plasticization due to the bonded oligomeric amphiphile. Therefore, combination of the above observations suggests that PS and P4VP[Zn(DBS)$_2$]$_{0.9}$ form alternating lamellae, which is not surprising as the weight fraction of the P4VP[Zn(DBS)$_2$]$_{0.9}$ block is $\varphi = 0.60$.[48] It is next studied whether there is another internal structure within the P4VP[Zn(DBS)$_2$] lamellae, in analogy with PS-*block*-P4VP hydrogen bonded to alkylphenols.[41] Figure 2c shows the X-ray scattering intensity curves in the q range of 0.06−2.00 Å^{-1}. Zn(DBS)$_2$ has peaks at q_1^*, $2q_1^*$, $3q_1^*$... indicating a lamellar structure with the long period of ca. 30 Å. PS-*block*-P4VP does not have peaks in this q range. The complex, in turn, has peaks at q_2^* and $2q_2^*$, which in combination with the FTIR, TEM, and SAXS data suggest an internal smaller structure within the P4VP[Zn(DBS)$_2$]$_{0.9}$ layers. The reason that its long period is only marginally larger than for pristine Zn(DBS)$_2$ is not yet known. The lamellar structure could be realized if P4VP and the coordinated polar $Zn^{2+}(SO_3^-)_2$ moieties form ionic layers whereas the dodecyl alkyl chains are extended and form the nonpolar layers.[37,47] Therefore, a hierarchical self-organization is proposed, i.e., lamellar-*within*-lamellar structure (see schematics in Figure 3). The smaller structure within the P4VP[Zn(DBS)$_2$]$_{0.9}$ domain was not resolved in TEM. Note also that the crystalline uncomplexed Zn(DBS)$_2$ has several peaks in the wide angle q range whereas the pure block copolymer and PS-*block*-P4VP[Zn(DBS)$_2$]$_{0.9}$ complex show only an amorphous halo, indicating that the crystallization is suppressed when Zn(DBS)$_2$ is attached to the P4VP.

To demonstrate concepts for pores of different sizes, complexes based on a smaller molecular weight block copolymer were also prepared, i.e., $M_{n,PS} = 41\ 400$ g/mol

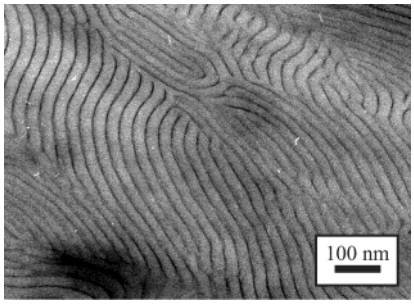

Figure 4. TEM micrograph of PS-*block*-P4VP[Zn(DBS)$_2$]$_{0.8}$ illustrating the lamellar structure with a long period ca. 250 Å. The P4VP[Zn(DBS)$_2$]$_{0.8}$ domain shows dark in the image due to I_2 staining. Thicknesses of PS and P4VP[Zn(DBS)$_2$]$_{0.8}$ lamellae are ca. 200 and 50 Å, respectively ($M_{n,PS}$ = 41 400 g/mol, $M_{n,P4VP}$ = 1900 g/mol).

and $M_{n,P4VP}$ = 1900 g/mol. Figure 4 shows a TEM micrograph of PS-*block*-P4VP[Zn(DBS)$_2$]$_{0.8}$, indicating a lamellar structure with the long period of ca. 250 Å. Also in this case, there is no common alignment of the lamellae, and a considerable number of defects remain in the sample. Interestingly, lamellar morphology is observed even if the weight fraction of P4VP[Zn(DBS)$_2$]$_{0.8}$ domain is $\varphi = 0.23$, and cylindrical morphology could be expected on the basis of simple diblock copolymer considerations.[48] This indicates an asymmetric phase diagram, as was observed also in PS-*block*-P4VP hydrogen bonded with alkylphenols.[41] The thicknesses of the PS and P4VP[Zn(DBS)$_2$]$_{0.8}$ lamellae are ca. 200 and 50 Å, which qualitatively agrees with the P4VP[Zn(DBS)$_2$]$_{0.8}$ weight fraction. Figure 5a represents the SAXS intensity curves for the scattering vector magnitudes of $q = 0.01-0.10$ Å^{-1}, and neither Zn(DBS)$_2$ nor PS-*block*-P4VP shows intensity maxima in this q range. The P4VP block is very short in this block copolymer (its weight fraction φ is only 4.4%), and it does not come as a surprise that no peaks due to order are observed for the pure PS-*block*-P4VP. For complexes y = 0.8 and 0.6, the relatively broad first intensity maxima are observed at q_1 = 0.023 and 0.028 Å^{-1} as well as faint indications for the second-order peaks at $2q_1$. These results agree with the lamellar order with long periods of 270 and 220 Å, respectively.

Figure 5b illustrates the SAXS intensity patterns for $q = 0.06-0.60$ Å^{-1}. In this q range, the first two peaks of Zn(DBS)$_2$ are observed due to the lamellar structure with long period of ca. 30 Å. The pure diblock copolymer, in turn, does not have any maximum in this q range. For complexes with y = 0.8 and 0.6, broad peaks at q = 0.20 Å^{-1} are observed, and no clear indications of the higher-order peaks are observed. Note that the order within the P4VP[Zn(DBS)$_2$]$_y$ layers is now much poorer than for the high molecular weight PS-*block*-P4VP[Zn(DBS)$_2$]$_y$ (Figure 2c). We suggest that it may be due to the thin P4VP[Zn(DBS)$_2$]$_y$ layers, as there are only 18 pyridine rings in the layers due to the short P4VP chains, and the closeness of the interfaces may disturb the structure formation.

Having established that PS-*block*-P4VP[Zn(DBS)$_2$]$_y$ forms lamellar structures, we wanted to study whether the oligomeric Zn(DBS)$_2$ amphiphiles could be extracted from the lamellae, leaving at least partially open pores. The underlying hypothesis was that the glassy PS phase and the relatively high number of defects would stabilize the structure and prevent it from collapsing. The result of the extraction was studied using FTIR, SAXS, and TEM.

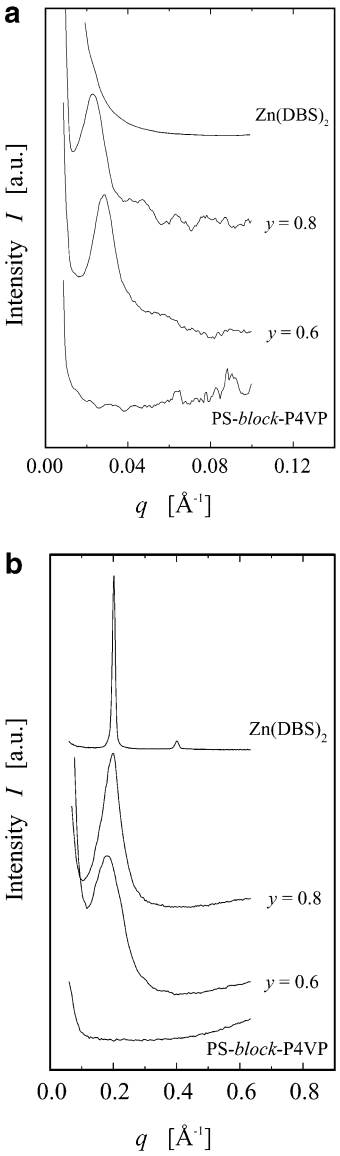

Figure 5. SAXS intensity patterns for Zn(DBS)$_2$, PS-*block*-P4VP[Zn(DBS)$_2$]$_y$, and PS-*block*-P4VP in the (a) $q = 0.01-0.10$ Å^{-1} and (b) $q = 0.06-0.60$ Å^{-1} regions. ($M_{n,PS}$ = 41 400 g/mol, $M_{n,P4VP}$ = 1900 g/mol). The intensity scale is linear.

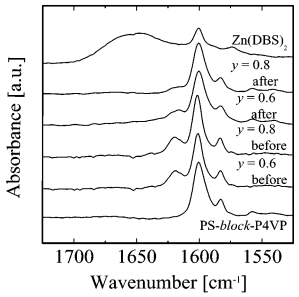

Figure 6. FTIR bands for Zn(DBS)$_2$, PS-*block*-P4VP[Zn(DBS)$_2$]$_y$, and PS-*block*-P4VP before and after Zn(DBS)$_2$ methanol extraction. In the complexes the characteristic band for pyridine coordination at 1619 cm^{-1} is significantly diminished, indicating that a substantial amount of Zn(DBS)$_2$ is removed from the material. In this case y only denotes the degree of complexation before Zn(DBS)$_2$ removal.

Figure 6 shows the FTIR spectra before and after the methanol extraction for selected samples. The characteristic band for the pyridine coordination at 1619 cm^{-1} is significantly diminished due to the methanol extrac-

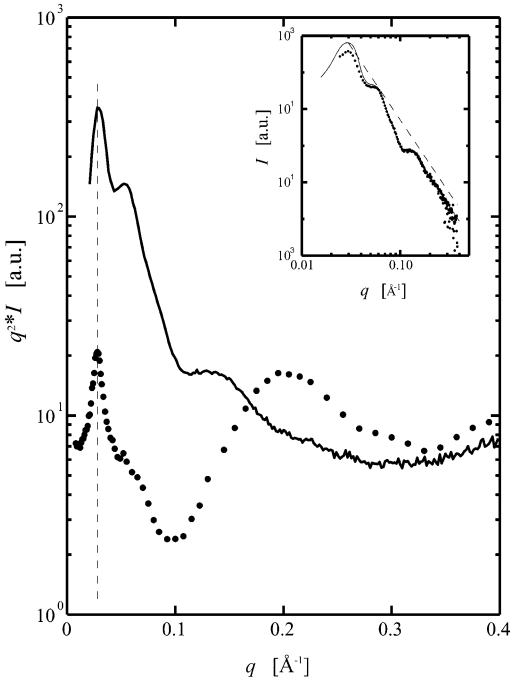

Figure 7. SAXS intensity patterns for PS-*block*-P4VP[Zn(DBS)$_2$]$_{0.60}$ before (dots) and after (solid line) Zn(DBS)$_2$ removal ($M_{n,PS}$ = 41 400 g/mol, $M_{n,P4VP}$ = 1900 g/mol). The intensity maximum corresponding to the internal structure within the P4VP[Zn(DBS)$_2$]$_{0.60}$ domain (ca. q = 0.20 Å^{-1}) disappears due to the removal of Zn(DBS)$_2$. Higher-order peaks corresponding to the block copolymer structure are also resolved more clearly in the extracted sample, possibly due to the enhanced electron scattering density difference. The long period was not affected by the methanol extraction. The inset illustrates that the data are fitted remarkably well with the ideal lamellar model as given by the solid curve. This model features infinite parallel lamellae with a long period of ca. 210 Å.

tion, indicating that a substantial amount of Zn(DBS)$_2$ is removed from the material. Further evidence for the amphiphile removal was observed based on the SAXS data. Figure 7 represents the SAXS intensity patterns before (dots) and after (solid line) the methanol treatment of PS-*block*-P4VP[Zn(DBS$_2$)]$_{0.6}$ ($M_{n,PS}$ = 41 400 g/mol, $M_{n,P4VP}$ = 1900 g/mol). The broad intensity maximum of the inner structure (q = 0.20 Å^{-1}) disappears upon methanol extraction, showing that a substantial part of the Zn(DBS)$_2$ has been removed. The long period corresponding to the block copolymer structure (q^* = 0.028 Å^{-1}, L_p = 220 Å) does not change upon extraction, indicating that the lamellar structure is retained. Importantly, higher-order peaks are also resolved more clearly in the extracted sample, as could be expected due to the enhanced electron scattering density difference. Note that if the structure would collapse upon extraction, the scattering electron density difference would decrease and the first-order peak could be more difficult to distinguish (see pure PS-*block*-P4VP in Figure 5a).

Finally, TEM was used to analyze the porosity of the high molecular weight complexes as the structures were expected to be more clearly resolvable in this case. Figure 2a already showed the lamellar structure before methanol extraction. The P4VP[Zn(DBS$_2$)]$_{0.9}$ domains show dark in the image due to the I_2 staining, but sufficient contrast was achieved even without staining due to the higher electron density of Zn^{2+}. Parts A and B of Figure 8 show the methanol-extracted samples without and with I_2 staining, respectively. First, the

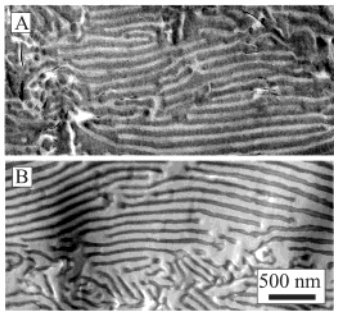

Figure 8. (A) Lamellar structure for the methanol extracted and unstained sample, where the electron deficient P4VP/air domain is now white. (B) Extracted and I_2-stained sample where the P4VP domain shows dark due to the increased electron density in that domain. It should be noted that if the amphiphiles were not removed, the P4VP[Zn(DBS$_2$)]$_{0.9}$ domain would always be dark in the images, with or without staining. The contrast inversion manifests most clearly in the "hairpin-like" defects ($M_{n,PS}$ = 238 100 g/mol, $M_{n,P4VP}$ = 49 500 g/mol).

relative thicknesses of the layers have not essentially changed during the methanol extraction, indicating that the structure remains and does not collapse. Second, the removal of Zn(DBS)$_2$ is confirmed by the "contrast inversion" in Figure 8A,B. The extracted and unstained sample is shown in Figure 8A, where the electron-deficient P4VP/air domain is now white. When the sample is stained with I_2 vapor, the P4VP domain turns to dark (Figure 8B) due to the increased electron density in that domain. The contrast inversion manifests more clearly in the "hairpin-like" defects. It should be noted that if the amphiphiles were not removed, the P4VP-[Zn(DBS$_2$)]$_{0.9}$ domain was always dark in the images, with or without staining.

Astonishingly, despite the relatively open lamellar structure, at least partially open pores can be prepared upon extraction of Zn(DBS)$_2$, probably stabilized due to the glassy PS phase, the different orientations of the lamellae, and the defects of the lamellar structure. A question remains on the more detailed structure of the pores. The resolution of TEM was not sufficient to give hints in this respect even for the large molecular weight (Figure 8A,B). However, the inset of Figure 7 illustrates for the methanol extracted sample PS-*block*-P4VP[Zn(DBS$_2$)]$_{0.6}$ that the overall X-ray scattering intensity follows Porod's law (q^{-4}) to at least q = 0.30 Å^{-1}. This suggests that the interfaces between pore and polymer are in fact sharp, and the boundary layer thickness is only of the order of few angstroms.[49] This may suggest that upon removal the amphiphiles the residual essentially uncomplexed P4VP brushes would line the pore walls (see scheme in Figure 9). So far, such a conclusion remains somewhat open, and the schematic picture has to be considered with some care.

4. Conclusion

We have demonstrated that self-organization of coordinated comb-shaped supramolecular templates can be used for preparation of mesoporous structures in a glassy PS medium. Compared to hydrogen bonding based on for example phenols, coordination allows bonding of higher molecular weight amphiphiles due to the stronger attraction. This, in turn, enables to prepare materials with larger porosity. Part of the supramolecular template, Zn(DBS)$_2$, can be removed using a selective solvent for P4VP and Zn(DBS)$_2$. This overcomes the need of having to use degradation or compa-

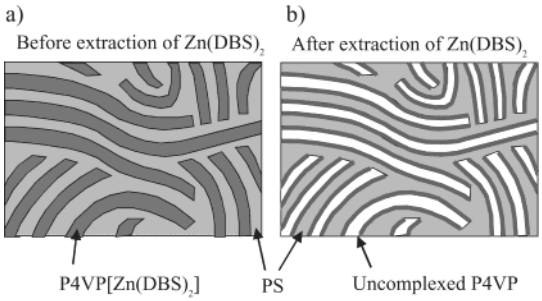

Figure 9. Schematics for lamellar mesoporous materials. (a) Lamellar structure before the amphiphile removal. The P4VP-$[Zn(DBS)_2]$ lamellae may contain another level of lamellar organization. (b) Proposed structure after the removal of Zn-$(DBS)_2$ with the residual P4VP brushes starting from the pore walls. Note that the internal structure of the pores is not yet known, and the shown scheme has to be regarded as tentative in this respect. Note also that the glassy PS matrix and imperfections in the alignment probably stabilize the mesoporous structure.

rable methods to produce porous materials. We found that the removal of the amphiphiles was successful, and the structures did not collapse, potentially due to the glassy PS phase, the different orientations of the nonaligned lamellae, and defects. This concept permits a relatively easy way to achieve structurally well-defined mesoporous materials with a narrow distribution of pore sizes with very high density of pores and high surface area per volume unit. In addition, upon proper selection of the blocks of the block copolymer and composition, it may be possible to increase the functionality and to get responsive brushes at the pore walls. We expect that such materials could be further developed to mesoscale electrical or biotechnological applications.

Acknowledgment. Dr. Riikka Mäki-Ontto is acknowledged for numerous discussions and experimental assistance. The financial support from the Academy of Finland and National Technology Agency (Finland) is gratefully acknowledged. This work made use of UCSB Material Research Laboratory Central Facilities supported by the National Science Foundation under Award DMR00-80034. This work was carried out in the Centre of Excellence of Finnish Academy ("Bio- and Nanopolymers Research Group", 77317). The Department of Electron Microscopy at the Institute of Biotechnology of University of Helsinki is acknowledged for the use of their facilities.

References and Notes

(1) Martin, C. R. *Chem. Mater.* **1996**, *8*, 1739.
(2) Beginn, U. *Adv. Mater.* **1998**, *10*, 1391.
(3) Batten, S. R.; Robson, R. *Angew. Chem., Int. Ed.* **1998**, *37*, 1460.
(4) Nangia, A. *Curr. Opin. Solid State Mater. Sci.* **2001**, *5*, 115.
(5) Jérôme, C.; Demoustier-Champagne, S.; Legras, R.; Jérôme, R. *Chem.—Eur. J.* **2000**, *6*, 3089.
(6) Martin, C. R.; Nishizawa, M.; Jirage, K.; Kang, M.; Lee, S. B. *Adv. Mater.* **2001**, *13*, 1351.
(7) Kresge, C. T.; Leonowicz, M. E.; Roth, W. J.; Vartuli, J. C.; Beck, J. S. *Nature (London)* **1992**, *359*, 710.
(8) Monnier, A.; Schüth, F.; Huo, Q.; Kumar, D.; Margolese, D.; Maxwell, R. S.; Stucky, G. D.; Krishnamurty, M.; Petroff, P.; Firouzi, A.; Janicke, M.; Chmelka, B. F. *Science* **1993**, *261*, 1299.
(9) Huo, Q.; Margolese, D. I.; Ciesla, U.; Feng, P.; Gier, T. E.; Sieger, P.; Leon, R.; Petroff, P. M.; Schüth, F.; Stucky, G. D. *Nature (London)* **1994**, *368*, 317.
(10) Lehn, J.-M. *Supramolecular Chemistry*; VCH: Weinheim, 1995.
(11) Russell, V. A.; Ward, M. D. *Chem. Mater.* **1996**, *8*, 1654.
(12) Russell, V. A.; Evans, C. C.; Li, W.; Ward, M. D. *Science* **1997**, *276*, 575.
(13) Gudbjartson, H.; Biradha, K.; Poirier, K. M.; Zaworotko, M. J. *J. Am. Chem. Soc.* **1999**, *121*, 2599.
(14) Chui, S. S.-Y.; Lo, S. M.-F.; Charmant, J. P. H.; Orpen, A. G.; Williams, I. D. *Science* **1999**, *283*, 1148.
(15) Müller, T.; Hulliger, J.; Seichter, W.; Weber, E.; Weber, T.; Wübbenhorst, M. *Chem.—Eur. J.* **2000**, *6*, 54.
(16) Seo, J. S.; Whang, D.; Lee, H.; Jun, S. I.; Oh, J.; Jeon, Y. J.; Kim, K. *Nature (London)* **2000**, *404*, 982.
(17) Kurth, D. G.; Fromm, K. M.; Lehn, J.-M. *Eur. J. Inorg. Chem.* **2001**, *6*, 1523.
(18) Su, C.-Y.; Yang, X.-P.; Kang, B.-S.; Mak, T. C. W. *Angew. Chem., Int. Ed.* **2001**, *40*, 1725.
(19) Dinolfo, P. H.; Hupp, J. T. *Chem. Mater.* **2001**, *13*, 3113.
(20) Templin, M.; Franck, A.; Du Chesne, A.; Leist, H.; Zhang, Y.; Ulrich, R.; Schädler, V.; Wiesner, U. *Science* **1997**, *278*, 1795.
(21) Göltner, C. G.; Henke, S.; Weissenberger, M. C.; Antonietti, M. *Angew. Chem., Int. Ed.* **1998**, *37*, 613.
(22) Simon, P. F. W.; Ulrich, R.; Spiess, H. W.; Wiesner, U. *Chem. Mater.* **2001**, *13*, 3464.
(23) Zhao, D.; Feng, J.; Huo, Q.; Melosh, N.; Fredrickson, G. H.; Chmelka, B. F.; Stucky, G. D. *Science* **1998**, *279*, 548.
(24) Hawker, C. J.; Hedrick, J. L.; Miller, R. D.; Volksen, W. *MRS Bull.* **2000**, *25*, 54.
(25) Bognitzki, M.; Hou, H.; Ishaque, M.; Frese, T.; Hellwig, M.; Schwarte, C.; Schaper, A.; Wendorff, J. H.; Greiner, A. *Adv. Mater.* **2000**, *12*, 637.
(26) Thurn-Albrecht, T.; Schotter, J.; Kästle, G. A.; Emley, N.; Shibauchi, T.; Krusin-Elbaum, L.; Guarini, K.; Black, C. T.; Tuominen, M. T.; Russell, T. P. *Science* **2000**, *290*, 2126.
(27) Xu, T.; Kim, H.-C.; DeRouchey, J.; Seney, C.; Levesque, C.; Martin, P.; Stafford, C. M.; Russell, T. P. *Polymer* **2001**, *42*, 9091.
(28) Jenekhe, S. A.; Chen, X. L. *Science* **1999**, *283*, 372.
(29) Widawski, G.; Rawiso, B.; Francois, B. *Nature (London)* **1994**, *369*, 387.
(30) Francois, B.; Pitois, O.; Francois, J. *Adv. Mater.* **1995**, *7*, 1041.
(31) Miller, S. A.; Kim, E.; Gray, D. H.; Gin, D. L. *Angew. Chem., Int. Ed.* **1999**, *38*, 3022.
(32) Beginn, U.; Zipp, G.; Möller, M. *Adv. Mater.* **2000**, *12*, 510.
(33) Beginn, U.; Zipp, G.; Mourran, A.; Walther, P.; Möller, M. *Adv. Mater.* **2000**, *12*, 513.
(34) Lee, H.-K.; Lee, K.; Ko, Y. H.; Chang, Y. J.; Oh, N.-K.; Zin, W.-C.; Kim, K. *Angew. Chem., Int. Ed.* **2001**, *40*, 2669.
(35) Mäki-Ontto, R.; de Moel, K.; de Odorico, W.; Ruokolainen, J.; Stamm, M.; ten Brinke, G.; Ikkala, O. *Adv. Mater.* **2001**, *13*, 117.
(36) Antonietti, M.; Conrad, J.; Thünemann, A. *Macromolecules* **1994**, *27*, 6007.
(37) Ruokolainen, J.; Tanner, J.; ten Brinke, G.; Ikkala, O.; Torkkeli, M.; Serimaa, R. *Macromolecules* **1995**, *28*, 7779.
(38) Ruokolainen, J.; Tanner, J.; Ikkala, O.; ten Brinke, G.; Thomas, E. L. *Macromolecules* **1998**, *31*, 3532.
(39) Kosonen, H.; Ruokolainen, J.; Knaapila, M.; Torkkeli, M.; Jokela, K.; Serimaa, R.; ten Brinke, G.; Bras, W.; Monkman, A. P.; Ikkala, O. *Macromolecules* **2000**, *33*, 8671.
(40) Ruokolainen, J.; Mäkinen, R.; Torkkeli, M.; Mäkelä, T.; Serimaa, R.; ten Brinke, G.; Ikkala, O. *Science* **1998**, *280*, 557.
(41) Ruokolainen, J.; ten Brinke, G.; Ikkala, O. *Adv. Mater.* **1999**, *11*, 777.
(42) Ikkala, O.; ten Brinke, G. *Science* **2002**, *295*, 2407.
(43) Agnew, N. H. *J. Polym. Sci., Polym. Chem. Ed.* **1976**, *14*, 2819.
(44) Peiffer, P. D.; Duvdevani, I.; Agarwal, P. K. *J. Polym. Sci., Polym. Lett. Ed.* **1986**, *24*, 581.
(45) Belfiore, L. A.; Pires, A. T. N.; Wang, Y.; Graham, H.; Ueda, E. *Macromolecules* **1992**, *25*, 1411.
(46) Hargreaves, A. *Acta Cryst.* **1957**, *10*, 191.
(47) Motamedi, F. *Liq. Cryst.* **1997**, *22*, 749.
(48) Bates, F. S.; Fredrickson, G. H. *Phys. Today* **1999**, *52*, 32.
(49) Baltá-Calleja, F. J.; Vonk, C. G. *X-Ray Scattering of Synthetic Polymers*; Elsevier: Amsterdam, 1989.

MA020538K